

****FULL TITLE****
*ASP Conference Series, Vol. **VOLUME**, **YEAR OF PUBLICATION***
****NAMES OF EDITORS****

Accretion and ejection in Sgr A*

Feng Yuan

*Shanghai Astronomical Observatory, Chinese Academy of Sciences, 80
 Nandan Road, Shanghai 200030, China; fyuan@shao.ac.cn*

Abstract.

We review our current understanding to the accretion and ejection processes in Sgr A*. Roughly speaking, they correspond to the quiescent and flare states of the source respectively. The high-resolution *Chandra* observations to the gas at the Bondi radius combined with the Bondi accretion theory, the spectral energy distribution from radio to X-ray, and the radio polarization provide us strict constraints and abundant information to the theory of accretion. We review these observational results and describe how the advection-dominated accretion flow model explains these observations. Recently more attentions have been paid to flares in Sgr A*. Many simultaneous multi-wavelength campaigns have been conducted, aiming at uncovering the nature of flares. The main observational properties of flares are briefly reviewed. Especially, the time lag between the peaks of flare at two radio frequencies strongly indicates that the flare is associated with ejection of radio-emitting blobs from the underlying accretion flow. Such kind of episodic jets is distinctive from the continuous jets and are quite common in black hole systems. We introduce the magnetohydrodynamical model for the formation of episodic jets recently proposed based on the analogy with the theory of coronal mass ejection in the Sun. We point out that the various observational appearances of flares should be explained in the framework of this model, since ejection and flare originate from the same physical process.

1. Introduction

Accretion onto compact objects is one of the most fundamental processes in the universe. It operates in various scales, ranging from the centers of almost each galaxies including our own, black hole and neutron star X-ray binaries, Gamma-ray bursts, to protostars. Among them the supermassive black hole in our Galaxy, Sgr A*, is unique because of its proximity (Schödel et al. 2002; Ghez et al. 2003). Sgr A* is one of the most strongest evidence for the existence of supermassive black holes. Because of this reason we have tremendously abundant data in various aspects, as we will describe below. This supplies us the most strict constraint to theoretical models.

In this review, we will focus on two aspects of Sgr A*. One is its quiescent state. The corresponding theory is black hole accretion. We will introduce the development of the advection-dominated accretion flow (ADAF) and illustrate how the main observations of the quiescent state of Sgr A* are naturally explained in this model. In fact, since its re-discovery in 1994, the model has been intensively studied via analytical work, numerical simulation, and comparison

with observations, so the ADAF model has been well established and become the standard model of low luminosity sources.

Another aspect we want to focus is flares of Sgr A*. This is a “hot spot” in recent years in Sgr A* community. Many simultaneous multi-waveband campaigns aiming at studying flares have been conducted successfully and valuable information have been obtained from them. As we will introduce below, these observations combined with some convincing theoretical works clearly indicate that the flares are physically associated with separate blob-like mass ejection from the accretion flow. We want to emphasize that this kind of mass ejection is different from the continuous jets we usually talk about. Rather, they are usually called “episodic jets”. Although the theoretical study of episodic jets is still in its infancy compared to the continuous jets, they are actually very common in black hole systems. We will introduce an MHD model for the formation of episodic jets which is recently proposed by analogy with the coronal mass ejection in the Sun (Yuan et al. 2009). We argue that flares in Sgr A* should be explained in the framework of this model.

2. Quiescent state of Sgr A*: the baseline model

2.1. Why unique? Observational constraints

The reason why Sgr A* is unique is because of its proximity. We therefore have abundant data which provides strict observational constraints on accretion models. Below we state the main constraints.

Outer boundary conditions. The accretion flow starts at the Bondi radius where the gravitational potential energy of the gas equals its thermal energy. For uniformly distributed matter with an ambient density ρ_0 and sound speed c_s , the Bondi radius of a black hole with mass M is $R_{\text{Bondi}} \approx GM/c_s^2$ and the mass accretion rate is $\dot{M}_{\text{Bondi}} \approx 4\pi R_{\text{Bondi}}^2 \rho_0 c_s$. The high spacial resolution of *Chandra* can well resolve the Bondi radius and these observations infer gas density and temperature as $\approx 100 \text{ cm}^{-3}$ and $\approx 2 \text{ keV}$ on $1''$ scales (Baganoff et al. 2003). The corresponding Bondi radius $R_{\text{Bondi}} \approx 0.04 \text{ pc} \approx 1'' \approx 10^5 R_s$ and $\dot{M}_{\text{Bondi}} \approx 10^{-5} M_\odot \text{ yr}^{-1}$. The 3D numerical simulation for the accretion of stellar winds onto Sgr A* by Cuadra et al. (2006) obtains $\dot{M} \approx 3 \times 10^{-6} M_\odot \text{ yr}^{-1}$, in good agreement with the estimation of the simple Bondi theory. This simulation also tells us that the angular momentum of the accretion flow at Bondi radius is not small, with the circularization radius being $\sim 10^4 R_s$. The Bondi radius, Bondi accretion rate, and the density, temperature, and the specific angular momentum of the gas at the Bondi radius constitute the outer boundary conditions that any accretion models must satisfy.

Spectral energy distribution. The spectral energy distribution of Sgr A* is shown in Fig. 1. The figure is directly taken from Yuan, Quataert & Narayan (2003), so some later observational data such as Genzel et al. (2003) and Schödel et al. (2007) are missing, but they do not affect our discussions here. The radio spectrum consists of two components. Below $\sim 86 \text{ GHz}$, the spectrum is described by a power-law form, while above this frequency we have a so-called “sub-millimeter bump”. This implies that the radio emission comes from two different components. The infrared (IR) observations always show some

variations which seems to indicate that there is no real quiescent state in IR band (Genzel et al. 2003; Ghez et al. 2004). The X-ray emission comes in two states, namely quiescent and flare ones, with different spectral index, as shown in Figure 1. A large fraction of the X-ray flux in the quiescent state is resolved, coming from an extended region. The bolometric luminosity of Sgr A* is only $L \approx 10^{36} \text{ erg s}^{-1} \approx 3 \times 10^{-9} L_{\text{Edd}}$. Combined with the Bondi accretion rate, this luminosity implies an extremely low radiative efficiency, $\eta \sim 10^{-6}$.

Polarization. A high level of linear polarization (2% \sim 10%) at frequencies higher than ~ 150 GHz was detected (e.g., Aitken et al. 2001; Bower et al. 2003, 2005; Macquart et al. 2006; Marrone et al. 2007), which sets the mean rotation measure to be $-5.6 \pm 0.7 \times 10^5 \text{ rad m}^{-2}$ (Marrone et al. 2007). This limits the accretion rate close to the black hole to less than $2 \times 10^{-7} M_{\odot} \text{ yr}^{-1}$ or $2 \times 10^{-9} M_{\odot} \text{ yr}^{-1}$, depending on the configuration of the magnetic field in the accretion flow¹. Such a mass accretion rate is much lower than the Bondi rate.

2.2. The standard thin disk is ruled out

The Bondi theory provides a good estimation to the accretion rate at the outer boundary. If the gas were accreted at this rate onto the black hole via the standard thin disk, the expected luminosity would be $L \approx 0.1 \dot{M}_{\text{Bondi}} c^2 \approx 10^{41} \text{ erg s}^{-1}$, five orders of magnitude higher than the observed luminosity. This is the strongest argument against a standard thin disk in Sgr A*. The second argument against this model is that the spectrum shown in Fig. 1 does not look like the multi-temperature blackbody spectrum predicted by a standard thin disk.

2.3. The advection-dominated accretion flow model

The equations of accretion onto a black hole allow two series of solutions, namely cool and hot ones. The standard thin disk model is the representative of the cool solution (another cool accretion solution corresponds to higher accretion rates and is “slim” disk). The temperature of the accretion flow in this solution is relatively low, $\sim 10^6 - 10^7 \text{ K}$. It is optically thick, geometrically thin (because of the low temperature), and radiatively efficient. This solution provides a good description to the big blue bump in the optical/UV band of the luminous AGNs (but see Koratkar & Blaes 1999) thus is believed to work in luminous AGNs.

The advection-dominated accretion flow belongs to the hot series (Narayan & Yi 1994, 1995; Abramowicz et al. 1995; see Narayan, Mahadevan & Quataert 1998 and Narayan & McClintock 2008 for reviews). In an ADAF, the temperature of ions is virial while the electron temperature is lower but still very high, $T_e \sim 10^9 - 10^{11} \text{ K}$. This solution is optically thin and geometrically thick. Most importantly, its radiative efficiency is typically much lower than that of the

¹Ballantyne, Özel, & Psaltis (2007) argue that since the electrons are relativistic over a large radii, polarized radiation from accretion flow will undergo generalized Faraday rotation, which will not depolarize the radiation even if the rotation measure is very high. Thus the polarization observations will not be able to constrain the accretion rate. However, the electrons are actually non-relativistic at radii larger than $\sim 100 r_s$ where most of the rotation measure is produced. On the observational side, the observed polarization angle varies as λ^2 (e.g., Macquart et al. 2006), which is what expected for Faraday rotation.

standard thin disk, $\eta_{\text{ADAF}} \approx 0.1\dot{M}/\dot{M}_{\text{crit}}$. Here $\dot{M}_{\text{crit}} \approx \alpha^2\dot{M}_{\text{Edd}}$ is the critical accretion rate of ADAF beyond which the ADAF solution fails and is replaced by another hot solution (“luminous hot accretion flow”).

The crucial point to modeling Sgr A* is that the accretion flow must be radiatively very inefficient. This is exactly the characteristic feature of an ADAF, as we emphasize above. In a standard thin disk, the viscously dissipated energy is radiated away locally, which results in a high efficiency. But in an ADAF, the radial velocity is much larger and the temperature is much higher than in a standard thin disk. Consequently, the density of the accretion flow is much lower. Therefore, the radiative timescale is much longer than the accretion timescale, thus most of the viscously dissipated energy is stored in the accretion flow as its thermal energy rather than being radiated away. This is the main reason for the low radiative efficiency of an ADAF. For the details of the dynamics of ADAFs, we refer the reader to the review of Narayan, Mahadevan & Quataert (1998) and Narayan & McClintock (2008).

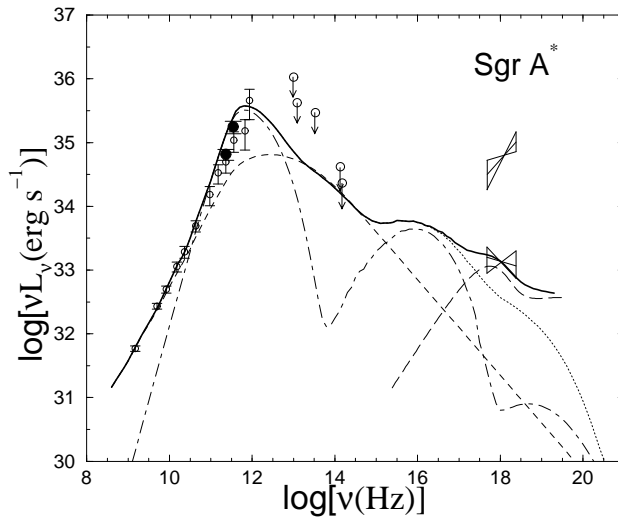


Figure 1. ADAF model for the quiescent state emission from Sgr A*. The dot-dashed line denotes the synchrotron and SSC emission by thermal electrons; the dashed line for the synchrotron emission by non-thermal electrons. The dotted line shows the total synchrotron and SSC emissions while the solid line also includes the bremsstrahlung emission from the outer parts of the ADAF (long-dashed line). From Yuan, Quataert & Narayan (2003).

Narayan, Yi & Mahadevan (1995) first apply the ADAF model to Sgr A*. They successfully explain the most important feature of the source, i.e., its low radiative efficiency. The spectrum has also been roughly explained. However, in the “old” ADAF model adopted in that paper, the mass accretion rate is assumed to be constant with radius. As a result, the rotation measure predicted in this model is much larger than that required from the polarization observation. This is a serious problem.

In the theoretical side, significant progresses on ADAFs have been made in the past decades. First, global, time-dependent, numerical simulations reveal that only a very small fraction of the mass available at large radii actually

accretes onto the black hole and most of it circulates in convective motions or is lost to a magnetically driven outflow (Stone, Pringle & Begelman 1999; Hawley & Balbus 2002). Second, in the old ADAF model, the turbulent dissipation is assumed to heat only ions. However, it was later realized that processes like magnetic reconnection is likely to heat electrons directly (Quataert & Gruzinov 1999; Sharma et al. 2007).

Yuan, Quataert & Narayan (2003) present a updated ADAF model to Sgr A*, taking into account the above-mentioned theoretical developments, i.e., outflow and direct electron heating by turbulent dissipation. Fig. 1 shows the spectral modeling result. Specifically, the sub-millimeter bump comes from the synchrotron emission of thermal electrons in the innermost region of the ADAF. Due to the convection, only about 1% of the gas available at the Bondi radius enters into the black hole horizon², so the density in the region close to the black hole is much lower than in Narayan et al. (1995). In this case, the rotation measure is much smaller and a high linear polarization is expected. The low-frequency radio and the IR emissions are assumed to be from some nonthermal electrons in the ADAF (since the plasma in ADAF is collisionless).

After the publication of Yuan et al. (2003), some new observations appeared. A notable one is the size measurement of Sgr A* at radio wavebands (Bower et al. 2004; Shen et al. 2005). These results supply independent test to theoretical models. Yuan, Shen & Huang (2006; see also Huang et al. 2007) calculated the predicted size of Sgr A* of Yuan et al. (2003) model and found good agreement with the observational results.

2.4. Comments on the two additional models for Sgr A*

In addition to the ADAF model, two competitive models are the jet model (Falcke, Mannheim & Biermann 1993; Falcke & Markoff 2000; Markoff et al. 2001; Yuan, Markoff & Falcke 2002; Markoff, Bower & Falcke 2007), and the spherical accretion model (Melia 1992; Melia, Liu & Coker 2000, 2001). Both models can explain the main observations well. In the jet model, most of the radiation in Sgr A* comes from synchrotron and synchrotron-self-Compton radiation of relativistic electrons accelerated in the jet. From a theoretical point of view, however, compared to accretion flows, there are much more uncertainties in a jet model in general. The mechanisms of launching and collimating jets have not been fully understood, thus large uncertainties exist about the structure of the jet and magnetic field in it. Regarding the electron acceleration, we are not sure whether they are accelerated by shock or magnetic reconnection, and many questions still have not been answered for both mechanisms. At last, if the radiation of Sgr A* is dominated by a jet, we have to explain why the radiation of the underlying accretion flow can be neglected, since the density and radiative efficiency in the accretion flow is usually higher than in a jet. Most importantly, so far we have not detected any jet in Sgr A* even though the proximity of the source and the high sensitivity of the radio telescope. This is the most serious challenge to the jet model.

²So the low efficiency of Sgr A* ($\eta \sim 10^{-6}$) is partly because of convection (10^{-2}) and partly because of energy advection (10^{-4}).

The spherical accretion model has many similar properties with an ADAF. In both models, the accretion flow is hot, with the temperature being virial. This is because both models are advection-dominated. This explains naturally why the radiative efficiency is so low, as required by observations. In both models, the main radiative process is the synchrotron emission by thermal electrons in the accretion flow, which is responsible for the sub-millimeter bump.

Two key differences exist between the spherical accretion model and ADAF. The first one is that in the former the specific angular momentum is assumed to be very low that the flow circularizes at a radius as small as 5-10 R_g . Thus the geometry of the accretion flow is an outer spherical accretion plus an inner small Keplerian disk. However, detailed numerical simulations to the accretion process in the Galactic center region indicates that the specific angular momentum of the gas is actually not small. The circularization radius is as large as $10^4 R_g$ (Cuadra et al. 2006). Another difference is that the spherical accretion model assume a one-temperature plasma while in an ADAF the ions are much hotter than electrons. Whether the plasma is two-temperature or not depends on the microphysics of the coupling between ions and electrons and is theoretically a difficult problem. Strong coupling mechanism has not been found so far. In this case, adiabatic compression should results in much hotter ions than electrons due to the difference of their adiabatic index. On the observational side, in the cases of supernova remnant and solar wind, the plasma is found to be two-temperature. At last, recent works seems to show that it is hard to fit the spectrum of Sgr A* if the accretion flow is one-temperature (Yuan et al. 2006; Mościbrodzka et al. 2009).

3. The flare activity and ejection of blobs from Sgr A*

3.1. Main properties of flares

Flares are detected in multi-wavebands, from radio, sub-millimeter, IR, to X-ray. At both IR and X-ray wavebands, the source is highly variable. The amplitude of the variability at IR is ~ 1 -5 (Genzel et al. 2003; Ghez et al. 2004). Fitting the spectrum with a power-law, $F_\nu \propto \nu^\alpha$, Hornstein et al. (2007) find that the spectral index α of IR flares is $\alpha = -0.6 \pm 0.2$, independent of the flux of the flares (but see Gillessen et al. 2006 for a different result). At X-ray band, the amplitude of the flare is typically higher, with amplitude as high as ~ 45 or even higher. The spectrum is quite diverse, with $\alpha = 0, 0.1, -0.3, -0.5, -1.5$ (Baganoff et al. 2001; Goldwurm et al. 2003; Porquet et al. 2003; Bélanger et al. 2005). The duration of the IR and X-ray flares are similar, typically 1-3 hours. The flare event usually occurs a few times per day. It is found that flares are the more seldom, the more luminous they are (Trippe et al. 2007; Yusef-Zadeh et al. 2009). In contrast to this, changes in the radio flux are limited to variations of $< 50\%$ within hours to days (e.g., Trippe et al. 2007; Yusef-Zadeh et al. 2008).

The flare emission is detected to be polarized in radio, sub-millimeter, and IR bands. In the radio band, compared to the quiescent state, the polarization degree is higher and the angle also changes (Yusef-Zadeh et al. 2008). The polarization degree at sub-millimeter band increases from 9% to 17% as the flare passes through its peak (Marrone et al. 2008). The IR flare is strongly

polarized, with degree of 20% or even up to 40% (Trippe et al. 2007; Eckart et al. 2008a). This is a strong evidence for a synchrotron origin of the flare emission.

A quasi-periodicity of ~ 20 minutes is claimed in the IR flares (Genzel et al. 2003; Eckart et al. 2006b; Meyer et al. 2006a, 2006b; Trippe et al. 2007; Zamaninasab et al. 2010), but this is a subject of substantial controversy (Meyer et al. 2008; Do et al. 2009).

3.2. Evidence for ejection of blobs

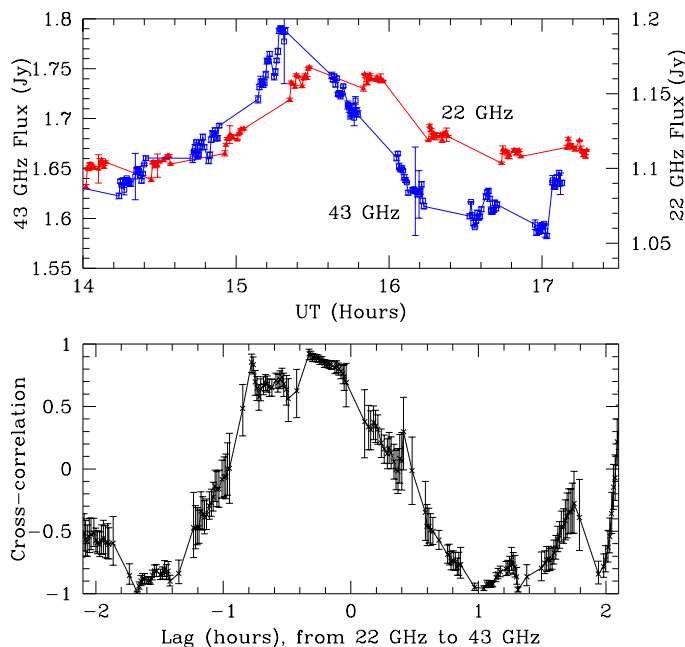


Figure 2. *Top:* Lightcurve of Sgr A* flare at 43 and 22 GHz. *Bottom:* The cross-correlation amplitude is shown as a function of lag time. From Yusef-Zadeh et al. (2006b).

Many simultaneous multi-waveband campaigns aimed at studying flares have been conducted and valuable information has been obtained (e.g., Eckart et al. 2006a; 2008b; Yusef-Zadeh et al. 2006a, 2008, 2009; Marrone et al. 2008). It is found that each X-ray flare is accompanied by an IR flare with zero time lag, but not vice versa. The timescales of the variability are quite similar, typically \sim an hour (Eckart et al. 2006a; Yusef-Zadeh et al. 2006a). The sub-millimeter flare is detected to lag the X-ray flare by 110 ± 17 minutes (Yusef-Zadeh et al. 2008; Marrone et al. 2008; Meyer et al. 2008). In the radio band, as shown by Figure 3, flares at 43 and 22 GHz are detected and it is found that the peak of 22 GHz flare lags that of the 43 GHz by 20-40 minutes (Yusef-Zadeh et al. 2006b, 2008).

Yusef-Zadeh et al. (2006b, 2008) argue that the time lag between 22 and 43 GHz, together with the rapid rise and slow decay of their light curves and the polarization of the flare, all can be naturally explained by a bubble of synchrotron-emitting electrons cooling via adiabatic expansion. The initial rise of the flux is because of the increase of the cross section of the blob when it is optically thick. With the expansion, the blob becomes optically thin, and the energy of electrons and the magnetic field both decrease, thus the emitted flux decreases. Because the (self-absorption) optical depth is a function of frequency and high-frequency emission becomes optically thin first with the expansion, this results in the lag of the 22 GHz peak compared to the 43 GHz one. This result tells us that the flares are physically associated with ejection of blobs from the accretion flow.

We would like to emphasize that the key point of this work is the isolated blob. Such kind of mass ejection is different from the continuous jet since it is episodic. In fact, so far we have not detected a continuous jet in Sgr A*, as we point out earlier.

3.3. An MHD model for the formation of episodic jets

Interestingly, episodic mass ejection from accretion flow are quite common and they are often called “episodic jets” (Fender & Belloni 2004). One evidence for episodic jets are the widely detected knots in jets of active galactic nuclei (AGNs). These knots are widely assumed to be due to collision of shells or blobs with different velocities (so the AGNs jets we detect are mixture of continuous and episodic mass outflows). In Galactic black holes, episodic jets are most easily detected during the transition from the hard X-ray spectral state to the soft X-ray spectral state. The ejection of matter is often associated with brief and intense flares in radio, IR, and X-ray bands, as in the case of Sgr A* (Mirabel & Rodriguez 1994; Mirabel et al. 1998; Fender et al. 1999; Hjellming & Rupen 1995; Corbel et al. 2002).

The characteristics of episodic ejections and steady, continuous jets are distinguishable (see review by Fender & Belloni 2004). The feature of episodic jets is that their radio spectrum evolves rapidly. It is initially optically thick and then becomes optically thin. This is exactly what we have observed in the radio flares of Sgr A*, but in contrast to continuous jets whose radio spectrum is always optically thick. In addition, there is evidence that the emission from ejected plasmoids is more highly polarized than the emission from the continuous jets (Fender & Belloni 2004). This is again similar to the observations of Sgr A* in which the flare emission is more polarized than in the quiescent state.

A natural question is then what causes the formation of episodic jets. The formation of continuous jets has been intensively studied and models have been proposed. It is believed to be associated with the large-scale open magnetic field (e.g. Blandford & Znajek 1977; Blandford & Payne 1982). However, the formation of episodic jets remains an open question. Recently, by analogy with the coronal mass ejection in the Sun, a magnetohydrodynamical model was proposed and it is suggested to be associated with the closed magnetic fields (Yuan et al. 2009). Figure 3 is the schematic picture of the model. Loops of magnetic field emerge into the disc corona because of Park instability. Since their foot points are anchored in the accretion flow which is differentially rotating and turbulent, reconnections and flares occur subsequently (e.g., Blandford 2002).

The reconnection process changes the magnetic field topology (see Fig. 3a). It also redistributes the helicity and stores most of it in a flux rope floating in the disc corona, resembling what happens in the Sun. Initially the flux rope is in equilibrium by the forces of magnetic pressure and magnetic tension. The magnetic configuration continues to evolve. The system eventually loses the equilibrium, rapidly expelling the flux rope, and a long current sheet develops behind the break-away flux rope, as shown by Fig. 3b. Magnetic reconnection then occurs in the current sheet. The magnetic pressure force becomes much stronger than the tension force, thus the flux rope is propelled away from the accretion disc. Figure 4 shows our calculation result of the velocity evolution of the ejected blob in the case of Sgr A*. We can see that the blob is accelerated to $0.8c$ within about half a hour. The readers are referred to Yuan et al. (2009) for the details of calculation.

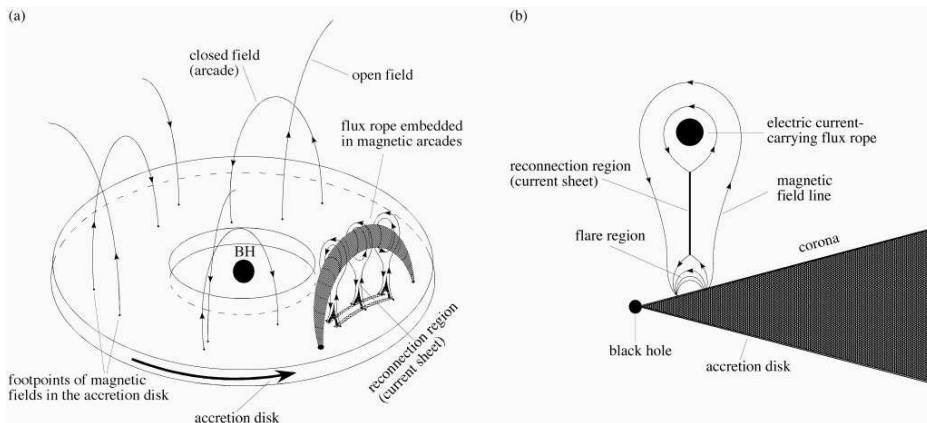


Figure 3. Illustration of the formation of a flux rope and its ejection. (a) Magnetic field emerges from the disc into the corona, and a flux rope is formed, as a result of the motion of the accretion flow and subsequent magnetic reconnection. (b) The flux rope is then ejected, forming a current sheet. Magnetic reconnection occurs subsequently, thus the magnetic tension becomes much weaker than the magnetic compression. This results in the energetic ejection of the blob. From Yuan et al. (2009).

3.4. Toward uncovering the mystery of flares

Several models have been proposed to explain the flares in Sgr A*. They include shock acceleration in jet (Markoff et al. 2001), magnetic reconnection in the accretion flow (Yuan, Quataert & Narayan 2004), turbulent acceleration in accretion flow (Liu et al. 2006a, 2006b), and “hot spot” model (Broderick & Loeb 2005) in which it is assumed that a localized region in the accretion flow brighten during the flare due to some reason. Most of these works are only phenomenological or they only focus on some aspects of the flare.

As indicated by the observations of flares in Sgr A*, and our knowledge of solar flare and coronal mass ejection in the Sun, the ejection of blobs is often associated with flares. This implies that the ejection and flare are basically two different appearance of the same physical process. Therefore, we should be

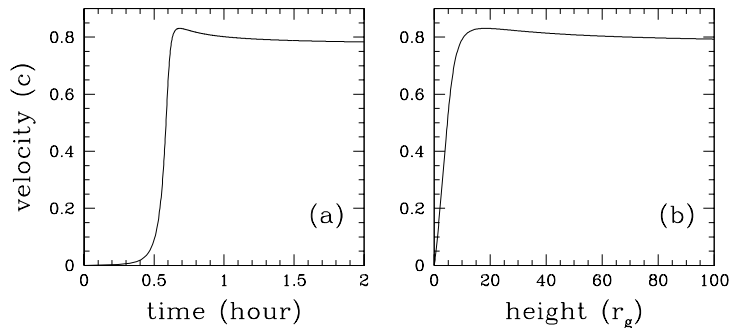


Figure 4. The calculated velocity of the ejected blob from Sgr A* as a function of time (a) and height (b). For comparison, the light-crossing time across r_g is ~ 20 s. From Yuan et al. (2009).

able to explain the flares in Sgr A* based on the “magnetic ejection” scenario introduced above. This work is still on-going (Yuan et al. in preparation). An analogy with solar flare should be valuable but significant differences are also expected due to the substantial difference of physical conditions in solar corona and disk corona. Important radiation should come from the relativistic electrons accelerated in the current sheet during the reconnection process (ref. Figure 3b). This radiation is likely to be responsible for the IR and X-ray flares. When the ejected blob propagates in the interstellar medium, the synchrotron emission from the blob itself and/or from the shock formed in front of the blob should be responsible for the radio and sub-millimeter flares. A time lag is naturally expected between the IR (or X-ray) flares and the radio or sub-millimeter ones. Because the magnetic field in the emission region is ordered and the emission is optically thin, a high degree of polarization is expected. As a comparison, for the quiescent state, the emission is likely to come from accretion flow where the magnetic field is more tangled and/or the emission is optically thick, so the polarization degree is lower.

4. Conclusion

The supermassive black hole in our Galactic center, Sgr A*, is the best laboratory to study the physics of black hole accretion. The main observational constraints include the mass accretion rate and the physical properties of the gas (temperature, density, and specific angular momentum) at the Bondi radius, the spectral energy distribution, and the polarization at radio wavebands. The advection-dominated accretion flow satisfies all these constraints and further is a well established theory for all low-luminosity sources.

More attention has been paid to the flares of Sgr A* in recent years. Many simultaneous multiwavelength campaigns have been conducted. From these observations especially the time lag between peaks of flares at different radio frequencies, we are now confident that blobs are ejected from the accretion flow during the flare. These episodic mass outflows are actually quite common in black hole systems and usually called episodic jets. Their observational appear-

ances are different from those of continuous jets in several important aspects such as spectrum and polarization. By analogy with the coronal mass ejection in the Sun, an MHD model has been proposed to explain the formation of episodic jets. Moreover, from the observations of flares in Sgr A* and the Sun, we know that the ejection of matter is often associated with them. In other words, ejection and flares are intrinsically different appearances of the same physical process. This implies that it is very promising that we are able to understand the flares in Sgr A* along this line.

Acknowledgments. This work was supported by the Natural Science Foundation of China (grants 10773024, 10833002, 10821302 and 10825314), Bairen Program of Chinese Academy of Sciences, and the National Basic Research Program of China (grants 2009CB824800 and 2006CB806303).

References

- Abramowicz, M.A., Chen, X., Kato, S., Lasota, J.-P., & Regev, O. 1995, *ApJ*, 438, L37
 Aitken, D.K. et al. 2000, *ApJ*, 534, L173
 Baganoff, F. K. et al., 2003, *ApJ*, 591, 891
 Baganoff, F. K., et al., 2001, *Nature*, 413, 45
 Ballantyne, D.R., Özel, F. & Psaltis, D. 2007, *ApJ*, 663, L17
 Bélanger et al. 2005, *ApJ*, 635, 1095
 Blandford R. D., 2002, in Gilfanov M., Sunyaev R., Churazov E., eds, *Lighthouse of the Universe: The Most Luminous Celestial Objects and Their Use for Cosmology*. Springer-Verlag, Berlin, p. 381
 Blandford R. D., Znajek R. L., 1977, *MNRAS*, 179, 433
 Blandford R. D., Payne D. G., 1982, *MNRAS*, 199, 883
 Bower, G.C. et al. 2003, *ApJ*, 588, 331
 Bower, G.C. et al. 2004, *Science*, 304, 704
 Bower, G.C. et al. 2005, *ApJ*, 618, L29
 Broderick, A. E., & Loeb, A. 2005, *MNRAS*, 363, 353
 Corbel S., et al. 2002, *Sci*, 298, 196
 Cuadra, J. et al. 2006, *MNRAS*, 366, 358
 Do, T. et al. 2009, *ApJ*, 691, 1021
 Eckart, A. et al. 2006a, *A&A*, 450, 535
 Eckart, A. et al. 2006b, *A&A*, 455, 1
 Eckart, A. et al. 2008a, *A&A*, 479, 625
 Eckart, A. et al. 2008b, *A&A*, 492, 337
 Falcke, H., Mannheim, K., & Biermann, P. L. 1993, *A&A*, 278, L1
 Falcke, H. & Markoff, S. 2000, *A&A*, 362, 113
 Fender R. P., & Belloni T. M., 2004, *ARA&A*, 42, 317
 Genzel. R. et al. 2003, *Nature*, 425, 934
 Ghez, A. M. et al. 2003, *ApJ*, 586, L127
 Ghez, A. M. et al. 2004, *ApJ*, 601, L159
 Gillessen, S. et al. 2006, *ApJ*, 640, L163
 Goldwurm, A. et al. 2003, *ApJ*, 584, 751
 Hawley, J. F. & Balbus, S. A. 2002, *ApJ*, 573, 738
 Hjellming R. M., & Rupen M. P., 1995, *Nat*, 375, 464
 Hornstein, S. et al. 2007, *ApJ*, 667, 900
 Huang, L., Cai, M., Shen, Z. & Yuan, F. 2007, *MNRAS*, 379, 833
 Koratkar, A., & Blaes, O. 1999, *PASP*, 755, 1
 Liu, S., Petrosian, V., & Mason, G.M. 2006a, *ApJ*, 634, 462
 Liu, S., et al. 2006b, *ApJ*, 648, 1020
 Macquart, J.P. et al. 2006, *ApJ*, 646, L111

- Manmoto, T. & Kato, S. 2000, PASJ, 538, 295
Maraschi, L. & Tavecchio, F. 2003, ApJ, 593, 667
Markoff, S., Falcke, H., Yuan, F. & Biermann, P. 2001, A&A, 379, L13
Markoff, S., Bower, G.C., & Falcke, H. 2007, MNRAS, 379, 1519
Marrone, D.P. et al. 2007, ApJ, 654, L57
Marrone, D.P. et al. 2008, ApJ, 682, 373
Melia, F. 1992, ApJ, 387, L25
Melia, F., Liu, S. & Coker, R. 2000, ApJ, 545, L117
Melia, F., Liu, S. & Coker, R. 2001, ApJ, 533, 146
Meyer L. et al. 2006a, A&A, 458, L25
Meyer L. et al. 2006b, A&A, 460, 15
Meyer L. et al. 2008, ApJ, 688, L17
Mirabel I. F., et al. 1998, A&A, 330, L9
Mirabel I. F., & Rodriguez L. F., 1994, Nat, 371, 46
Mościbrodzka, M. et al. 2009, ApJ, 706, 497
Mościbrodzka, M. et al. in this proceedings
Narayan, R. 2005, ApS&S, 300, 177
Narayan, R. & Yi, I. 1994, ApJ, 428, L13
Narayan, R. & Yi, I. 1995, ApJ, 444, 231
Narayan, R., Yi, I., & Mahadevan, R., 1995, Nature, 374, 623
Narayan, R., Mahadevan, R., & Quataert, E. 1998, in “The Theory of Black Hole Accretion Discs”, eds. M.A. Abramowicz, G. Bjornsson, and J.E. Pringle, (Cambridge University Press)
Narayan, R., & McClintock, J. E. 2008, NewAR, 51, 733
Porquet, D. et al. 2003, A&A, 407, L17
Quataert, E. & Gruzinov 1999, ApJ, 520, 248
Schödel, R. et al. 2002, Nature, 419, 694
Sharma, P., Quataert, E., Hammett, G. & Stone, J. 2007, ApJ, 667, 714
Shen, Z.-Q. et al. 2005, Nature, 438, 62
Stone, J., Pringle, J., & Begelman, M. 1999, MNRAS, 310, 1002
Trippe, S. et al. 2007, MNRAS, 375, 764
Yuan, F., Markoff, S., & Falcke, H., 2002, A&A, 383, 854
Yuan, F., Quataert, E., & Narayan, R. 2003, ApJ, 598, 301
Yuan, F., Quataert, E., & Narayan, R. 2004, ApJ, 606, 894
Yuan, F., Shen, Z.Q., Huang, L. 2006, ApJ, 642, L45
Yuan, F., Taam, R., Xue, Y., & Wu, X. 2006, ApJ, 636, 46
Yuan, F., Lin, J., Wu, K. & Ho, L.C. 2009, MNRAS, 395, 2183
Yusef-Zadeh, F. et al. 2006a, ApJ, 644, 198
Yusef-Zadeh, F. et al. 2006b, ApJ, 650, 189
Yusef-Zadeh, F. et al. 2008, ApJ, 682, 361
Yusef-Zadeh, F. et al. 2009, ApJ, 706, 348
Zamaninasab, M. et al. 2010, A&A, 510, A3